References and Notes

1. J. M. Tranquada, B. J. Sternlieb, J. D. Axe, Y. Nakamura, S. Uchida, *Nature* **375**, 561–563 (1995).
2. P. Abbamonte *et al.*, *Nat. Phys.* **1**, 155–158 (2005).
3. G. Ghiringhelli *et al.*, *Science* **337**, 821–825 (2012).
4. J. Chang *et al.*, *Nat. Phys.* **8**, 871–876 (2012).
5. R. J. Cava, A. Santoro, D. W. Johnson, W. W. Rhodes, *Phys. Rev. B* **35**, 6716–6720 (1987).
6. B. Büchner, M. Breuer, A. Freimuth, A. P. Kampf, *Phys. Rev. Lett.* **73**, 1841–1844 (1994).
7. E. Fradkin, S. A. Kivelson, *Nat. Phys.* **8**, 864–866 (2012).
8. H. Ding *et al.*, *Phys. Rev. Lett.* **78**, 2628–2631 (1997).
9. A. Damascelli, Z. Hussain, Z.-X. Shen, *Rev. Mod. Phys.* **75**, 473–541 (2003).
10. H. B. Yang *et al.*, *Nature* **456**, 77–80 (2008).
11. A. Mans *et al.*, *Phys. Rev. Lett.* **96**, 107007 (2006).
12. U. Chatterjee *et al.*, *Phys. Rev. Lett.* **96**, 107006 (2006).
13. J. E. Hoffman *et al.*, *Science* **297**, 1148–1151 (2002).
14. C. Howald, H. Eisaki, N. Kaneko, A. Kapitulnik, *Proc. Natl. Acad. Sci. U.S.A.* **100**, 9705–9709 (2003).
15. M. Vershinin *et al.*, *Science* **303**, 1995–1998 (2004).
16. T. Hanaguri *et al.*, *Nat. Phys.* **3**, 865–871 (2007).
17. W. D. Wise *et al.*, *Nat. Phys.* **4**, 696–699 (2008).
18. Y. Kohsaka *et al.*, *Nature* **454**, 1072–1078 (2008).
19. C. V. Parker *et al.*, *Nature* **468**, 677–680 (2010).
20. S. A. Kivelson *et al.*, *Rev. Mod. Phys.* **75**, 1201–1241 (2003).
21. E. H. da Silva Neto *et al.*, *Phys. Rev. B* **85**, 104521 (2012).
22. Materials and methods are available as supplementary materials on *Science* Online.
23. R. Comin *et al.*, *Science* **343**, XXX (2013).
24. T. Hanaguri *et al.*, *Science* **323**, 923–926 (2009).
25. Q.-H. Wang, D.-H. Lee, *Phys. Rev. B* **67**, 020511 (2003).
26. P. W. Anderson, N. P. Ong, *J. Phys. Chem. Solids* **67**, 1–5 (2006).
27. M. Randeria, R. Sensarma, N. Trivedi, F.-C. Zhang, *Phys. Rev. Lett.* **95**, 137001 (2005).
28. W. S. Lee *et al.*, *Nature* **450**, 81–84 (2007).
29. I. M. Vishik *et al.*, *Nat. Phys.* **5**, 718–721 (2009).

Acknowledgments: The work at Princeton was primarily supported by a grant from the U.S. Department of Energy (DOE) Basic Energy Sciences. The instrumentation and infrastructure at the Princeton Nanoscale Microscopy Laboratory used for this work were also supported by grants from NSF-DMR1104612, the NSF–Materials Research and Engineering Center program through Princeton Center for Complex Materials (DMR-0819860), the Eric & Wendy Schmidt Transformative Fund, and the W. M. Keck Foundation. Work at BNL was supported by DOE under contract DE-AC02-98CH10886. The Max Planck–UBC Centre for Quantum Materials and Canadian Insititute for Advanced Research Quantum Materials also supported this work. We thank P. W. Anderson, E. Abrahams, S. Kivelson, S. Misra, and N. P. Ong for fruitful discussions. We also acknowledge A. Damascelli and B. Keimer for discussions and for sharing the results of their x-ray studies on Bi-2201 before publication. A.Y. acknowledges the hospitality of the Aspen Center for Physics, supported under NSF grant PHYS-1066293. The synthesis of the oxygen-doped Bi2212 samples was supported by the Center for Emergent Superconductivity, an Energy Frontier Research Center.

Supplementary Materials

www.sciencemag.org/content/343/6169/393/suppl/DC1
Materials and Methods
Figs. S1 to S9
References (*30*, *31*)

19 July 2013; accepted 25 November 2013
Published online 19 December 2013;
10.1126/science.1243479

Imaging Dynamics on the $F + H_2O \rightarrow HF + OH$ Potential Energy Surfaces from Wells to Barriers

Rico Otto,[1]* Jianyi Ma,[2,3]* Amelia W. Ray,[1] Jennifer S. Daluz,[1] Jun Li,[3] Hua Guo,[3]† Robert E. Continetti[1]†

The study of gas-phase reaction dynamics has advanced to a point where four-atom reactions are the proving ground for detailed comparisons between experiment and theory. Here, a combined experimental and theoretical study of the dissociation dynamics of the tetra-atomic FH_2O system is presented, providing snapshots of the $F + H_2O \rightarrow HF + OH$ reaction. Photoelectron-photofragment coincidence measurements of the dissociative photodetachment (DPD) of the $F^-(H_2O)$ anion revealed various dissociation pathways along different electronic states. A distinct photoelectron spectrum of stable FH–OH complexes was also measured and attributed to long-lived Feshbach resonances. Comparison to full-dimensional quantum calculations confirms the sensitivity of the DPD measurements to the subtle dynamics on the low-lying FH_2O potential energy surfaces over a wide range of nuclear configurations and energies.

Thanks to the fruitful interplay between experiment and theory, our understanding of elementary atom-diatom reactions such as $F + H_2 \rightarrow HF + H$ at the quantum mechanical level is now highly sophisticated (*1*, *2*). As the number of atoms N in a chemical reaction increases, the complexity grows dramatically as $3N-6$ coordinates are necessary to fully describe the system. With six degrees of freedom, four-atom reactions have emerged naturally as the new proving ground for understanding reaction dynamics. Recently, theoretical methods have progressed to a level where highly accurate comparisons with experimental results are becoming possible for four-atom reactions (*3*), such as the benchmark $H_2 + OH \rightarrow H_2O + H$ and its isotopologs (*4*–*7*).

One of the key foundations for analyzing a chemical reaction is a detailed knowledge of the Born-Oppenheimer potential energy surface (PES), which represents the relation between a geometrical arrangement of the nuclei of a chemical system and its corresponding electronic energy. A number of experimental techniques have been developed that are sensitive to different aspects of the molecular PES. For example, rate coefficients depend on the height of reaction barriers and/or are sensitive to the long-range forces between reactants. Molecular spectroscopy provides structural information and allows probing of different product internal states. Crossed-molecular beam measurements of angle-resolved differential cross sections map the reaction dynamics on a quantum state-to-state level (*8*) and are sensitive to dynamical (e.g., Feshbach) resonances in chemical reactions (*9*). In addition, nonadiabatic dynamics that involve transitions between multiple electronic PESs have also attracted increasing attention (*10*, *11*). Negative ion photoelectron spectroscopy has been demonstrated as an effective tool (*12*) with application to both nonadiabatic effects (*13*) and resonance phenomena (*14*). The combined information from these different sources offers a stringent test for state-of-the-art theoretical methods, advancing our understanding of chemical reactions in more complex systems. Substantial progress in the field of reaction dynamics has thereby always been closely tied to the detailed study of benchmark systems like $F + H_2$. A natural extension to consider as we move to four-atom systems is the $F + H_2O$ reaction.

The $F + H_2O$ reaction is a prototypical hydrogen abstraction reaction between a radical and water. It represents a fundamental reaction of anthropogenic fluorine in Earth's atmosphere (*15*) and may also play a key role in the formation of HF that has recently been discovered in the interstellar media (*16*). The interaction of the F atom with water gives rise to three different PESs, two of which correlate with the $F(^2P_{3/2})$ ground state (Fig. 1). In the adiabatic limit, the lower-lying ground (X) state corresponds to $HF + OH(^2\Pi_{3/2})$, whereas the higher-lying excited (A) state leads to spin-orbit excited $HF + OH(^2\Pi_{1/2})$ products (*17*). A reaction barrier separates van der Waals (vdW) complexes on the entrance and exit channel sides of the reaction (*18*, *19*). Recent theoretical studies have shown that the prereaction

[1]Department of Chemistry and Biochemistry, University of California, San Diego, 9500 Gilman Drive, La Jolla, CA 92093, USA. [2]Institute of Atomic and Molecular Physics, Sichuan University, Chengdu, Sichuan 610065, China. [3]Department of Chemistry and Chemical Biology, University of New Mexico, Albuquerque, NM 87131, USA.

*These authors contributed equally to this work.
†Corresponding author. E-mail: hguo@unm.edu (H.G.); rcontinetti@ucsd.edu (R.E.C.)

complex, F–H_2O, may have a strong influence on the reactivity of the system (*20*).

An early study of the F + H_2O rate coefficient found no temperature dependence over a wide range, implying a tunneling-mediated reaction at low temperatures (*21*). Wang and co-workers have probed the transition state of the F + H_2O reaction using anion photoelectron spectroscopy at 6.42-eV photon energy (*22*), and the fragmentation process has been analyzed by direct dynamics simulations (*23*). In an extensive set of crossed beam experiments, Nesbitt and co-workers have explored the F + H_2O/D_2O reaction in great detail (*17*, *24*–*26*), using optical methods to probe the internal state distributions of the nascent diatomic products. Although the collision energies in these experiments were too low to overcome the adiabatic barrier for the formation of spin-excited OH, a branching ratio of $^2\Pi_{3/2}$:$^2\Pi_{1/2}$ = 0.69:0.31 was observed, suggesting the importance of nonadiabatic dynamics beyond the Born-Oppenheimer picture in this system (*25*).

Here, we report on a joint experimental and theoretical study of the FH_2O system. Unlike crossed beam experiments, where reaction products are only probed asymptotically, the photoelectron-photofragment coincidence experiment used here provides snapshots of the reaction dynamics all along the reaction coordinate, from the saddle point accessed by photodetachment to the asymptotic product channels as determined by translational spectroscopy. As shown in Fig. 1, the wave function for the $F^-(H_2O)$ anion has substantial overlap with configurations ranging from the saddle point to the vdW wells on the neutral reaction surface. This makes a comparison with state-of-the-art quantum dynamics calculations possible for a broad range of observables, illustrating the great strides being made in understanding the PES and dynamics of four-atom systems.

In the experiment, a pulsed laser at 258 nm (4.80 eV) was used to photodetach an electron from $F^-(H_2O)$ in a fast ion beam, and the photoelectron was collected in a velocity map imaging spectrometer. The photofragments resulting from this process were collected in coincidence on a

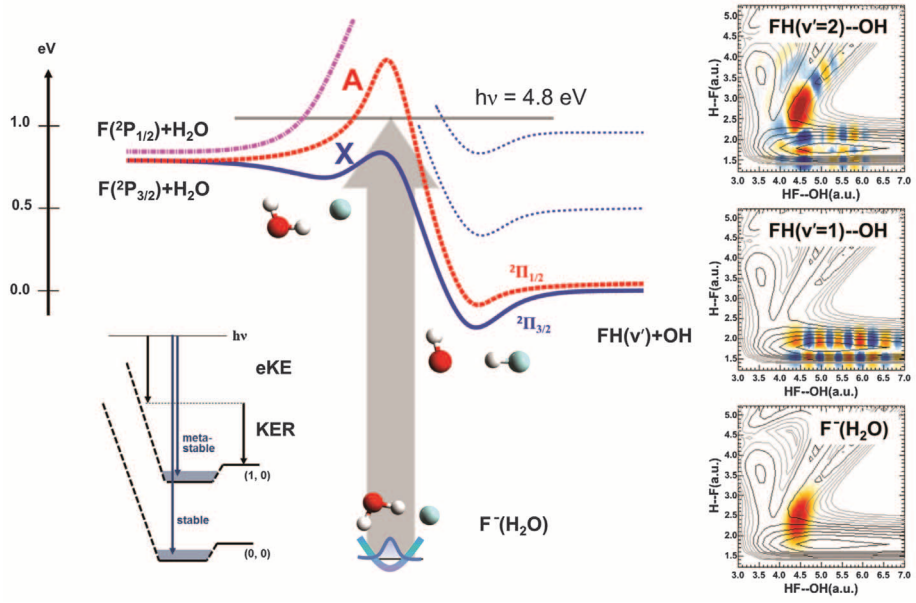

Fig. 1. Potential energy surfaces of the ground (X) and excited (A) states of the FH_2O system. In the PPC experiment, the $F^-(H_2O)$ anion (as indicated schematically) is projected onto the neutral surfaces by laser photodetachment. The energy of the ejected photoelectron (eKE) is measured in coincidence with the kinetic energy release of the photofragments (KER). A photoelectron spectrum of nondissociative events is measured by enforcing coincidence between electrons and stable FH_2O products only. The panels on the right show wave functions for the $F^-(H_2O)$ anion and Feshbach resonances for FH(v′ = 1)–OH and FH(v′ = 2)–OH states on the X state, with coordinates described in the SM. The energetic contours on the X state surface are spaced by 0.2-eV contours, with the darker contours representing energetically allowed regions at the photon energy used. The wave functions in the two Jacobi coordinates are obtained with other coordinates fixed at the maximal probability.

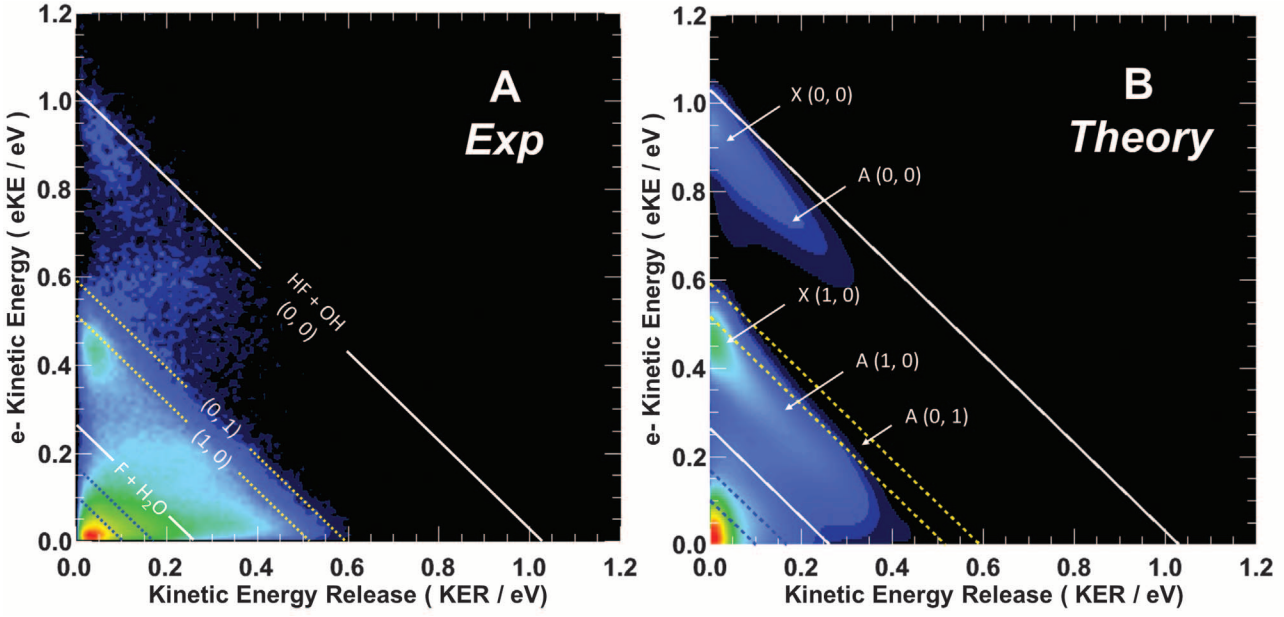

Fig. 2. Photoelectron-photofragment coincidence spectra for the FH_2O system. (**A**) Measured and (**B**) calculated spectra are compared. The solid white lines mark the energetic limits for dissociation into HF + OH (upper line) and F + H_2O (lower line) fragments. The dashed lines indicate vibrationally excited product states. White arrows in (B) show regions of notable contributions for specific channels.

time- and position-sensitive detector to determine the translational energy release from the dissociation. The photoelectron-photofragment-coincidence (PPC) technique allows the "half reaction" (i.e., the fragmentation into either reactants or products) to be measured in a kinematically complete fashion (*27*, *28*). The PPC spectrum was obtained by recording the electron kinetic energy (eKE) and photofragment kinetic energy release (KER) for each event in a two-dimensional (2D) coincidence plot (Fig. 2A). The overall energy available in the dissociative photodetachment (DPD) process can be distributed into either electron kinetic energy or photofragment energy (kinetic and internal). The total kinetic energy (hereafter simply called "total energy") determines the internal energy of the products, and therefore their final states. All combinations of eKE and KER that lead to the same final states give rise to a diagonal band structure that emerges from the spectrum. The maximum total energy available in the dissociation is given by the photon energy, the energy necessary to photodetach an electron from $F^-(H_2O)$, and the energy released in the fragmentation (*29*). HF + OH products reach this energetic cutoff when all available energy is converted into translational energy. This energetic cutoff is marked by the outermost diagonal white line in Fig. 2.

The PPC spectrum in Fig. 2 reveals many details of the dissociation dynamics. Although the experimental resolution is not sufficient to distinguish different rotational levels in the products, high rotational excitation can be inferred from the width of the observed vibrational bands. At total energies of 0.59 and 0.52 eV, formation of $HF(v' = 0) + OH(v' = 1)$ and $HF(v' = 1) + OH(v' = 0)$ products, denoted (0, 1) and (1, 0), respectively, becomes possible. These energetic limits are marked by the yellow dotted lines in the spectrum that assume single vibrational quanta in the OH and HF products. Both product states are observed as soon as they become energetically possible. Once these product channels open up along the eKE coordinate, the (0, 0) products die off, indicating that dissociative events starting from configurations close to the barrier for the reaction (at low eKE) favor production of vibrationally excited states. This HF vibrational excitation is a consequence of substantial lengthening of the H-F distance in the transition state relative to the equilibrium bond length of the free HF product.

The energetics for populating (0, 2), (2, 0), and (1, 1) final states are marked by the diagonal lines located at 0.18, 0.11, and 0.09 eV total energy, respectively. At a total energy of 0.25 eV, fragmentation into $F + H_2O$ becomes accessible, as marked by the lower white line in the image. Under the current experimental conditions, the $F + H_2O$ product channel cannot be separated from the formation of HF + OH owing to limited product mass resolution. Analyzing the vibrational state distributions, we find that only 8% of all products are observed in the (0, 0) ground state. A majority of all events (52%) are found in the energetic range between the opening of the (0, 1) and the (0, 2) product channels. This result is consistent with recent crossed beam experiments for the $F + H_2O$ reaction where a population inversion for the HF(v = 1) stretch mode was observed (*26*).

All events in the (0, 0) band are observed in two distinct regions of the PPC spectrum. One region is centered around high eKE (0.9 eV) and low KER (0.05 eV), the other around lower eKE (0.6 eV) and higher KER (0.2 eV). Both regions are found in a diagonal band structure representing the same total energy and therefore lead to the same final states. The pattern is mirrored in the (1, 0) band with a higher (0.45 eV) and a lower (0.15 eV) eKE region. This finding points to two different channels for the dissociation process and, as discussed below, reflects different electronic states that participate in the dissociation.

To test our ability to predict and understand the experimental results, we have modeled the dissociation process using full-dimensional quantum dynamics calculations, based on ab initio PESs of the two lowest-lying electronic states of FH_2O (Fig. 1) (*18*, *19*). Mimicking the experiment, the anion wave function in its ro-vibrational ground state on an ab initio–based anion PES is vertically projected on the neutral PESs and propagated with a full-dimensional Hamiltonian ($J = 0$). Both the $F + H_2O$ and HF + OH asymptotic states are resolved after propagation of ~2 ps. The final-state distributions at the photon energy are then used to construct the 2D PPC spectrum (see supplementary materials, SM). Overall, the agreement between the experimental data and theoretical results is very good (Fig. 2B). The topology of the spectrum, as well as the relative population of the various fragmentation channels, is well reproduced, indicating that the theory captures the essence of the dynamics of FH_2O dissociation. The calculations allow decomposition of the PPC spectrum into its final-state resolved components (figs. S2 to S4), which sheds further light on the features observed in the experiment. Indeed, the theoretical results confirm the large preponderance of (1, 0) products (66% of all products at this photon energy), in agreement with the experimental results. The outgoing wave function becomes temporarily trapped in a number of Feshbach resonance states (Fig. 1). This resonance-mediated dissociation is directly correlated with vibrationally excited HF products. In addition, the theoretical results confirm that the A state plays a substantial role in the dissociation dynamics of FH_2O and is responsible for the weak features, with low eKE and high KER in each channel. By contrast, the fraction for the $F + H_2O$ channel is found to be small (12%) and exclusively originates from the X state.

Complementary to the dissociative channels, long-lived complexes in the FH_2O system were identified by enforcing coincidence of the outgoing photoelectron with single particles arriving at the neutral detector with the mass of the parent anion, yielding a photoelectron spectrum of stable neutral complexes (Fig. 3). This kind of information cannot be obtained in a photoelectron spectroscopy measurement, where the fate of the neutral products is not recorded. The existence of such a spectrum in the FH_2O system is per se quite remarkable as any metastable states must have a lifetime of $\gtrsim$5 μs to be detectable in the experiment. The observed stable spectrum in Fig. 3 features a double peak structure at 1.0 and 1.15 eV.

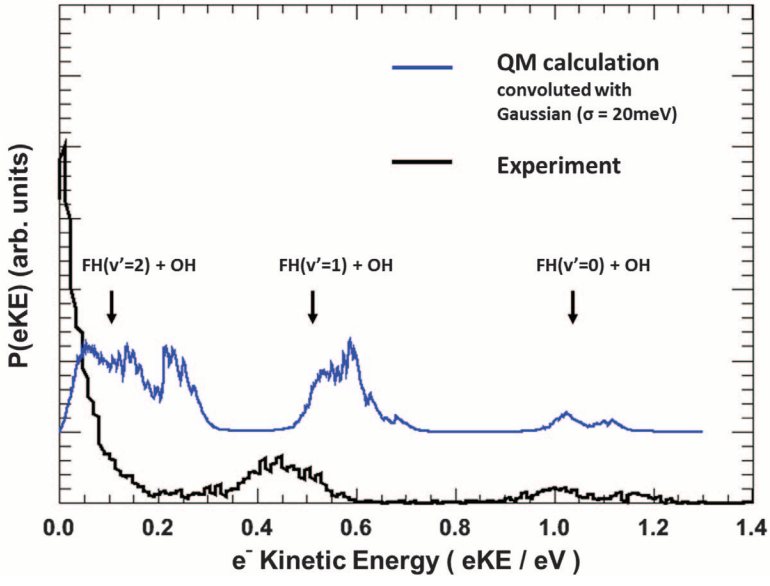

Fig. 3. Experimental and theoretical stable photoelectron spectra for the FH_2O system, showing the normalized electron probability distribution as a function of eKE. The peaks in both spectra at ~1.15 eV are assigned to a direct transition into bound states in the stable FH–OH vdW well. The peaks at ~0.5 eV in both spectra are assigned to Feshbach resonance states trapped in the FH(v′ = 1)–OH vdW well. QM, quantum mechanical.

The peak associated with the highest eKE in the spectrum is found beyond the energetic limit for fragmentation into OH + HF ground state products. These events must result from direct photodetachment into the exit channel FH–OH vdW complex of the F + H_2O reaction. A higher-lying HF–HO vdW complex in the exit channel may be responsible for the lower-energy peak at 1.0 eV (*19*). Another feature is observed at 0.45 eV, roughly one vibrational quantum in HF (~0.6 eV) above the FH–OH vdW complex. Corresponding features observed in the dissociative PPC spectrum in Fig. 2 suggest that this signal arises from a temporarily trapped vdW complex, FH(v′ = 1)–OH, a long-lived Feshbach resonance.

To understand the nature of the stable spectrum, the energy spectrum of the remaining wave packet after 2.5-ps propagation was computed. The calculated spectrum is compared in Fig. 3 with the experiment. The features centered around 0.55 and 0.15 eV are attributed to long-lived Feshbach resonances trapped in the FH(v′ = 1,2)–OH vdW wells, with representative wave functions illustrated in Fig. 1. Given that the experimental spectrum represents states with far longer lifetimes (5 μs) than is tractable to theoretically compute, the agreement is quite reasonable. An intriguing finding is the peak at 0.05 eV in the calculated stable spectrum. A closer inspection of the coincidence plot in Fig. 2A reveals a corresponding horizontal feature at the same eKE, corresponding to events distributed between KER = 0 to 0.4 eV. The appearance of this feature in conjunction with the peak observed in the stable spectrum can be interpreted in terms of a metastable state that is formed in the DPD process [e.g., an FH(v′ = 2)–OH Feshbach resonance] and therefore has a fixed electron spectrum. However, as this state decays on its way to the detector, the delayed fragmentation process over a nanosecond-microsecond time scale leads to an underestimation of the KER of the fragments, resulting in a horizontal band structure.

The wide range of observables simultaneously captured in the PPC experiment reported here provides a critical test for the accurate description of both the PESs and reaction dynamics over a wide range of translational and internal energies. Both lowest-lying electronic states play an active role in the dissociation process and must be taken into account to understand the nature of the FH_2O dissociation. Long-lived Feshbach resonances have been found in this four-atom system, experimentally and theoretically. Although very good overall agreement has been achieved between experiment and theory, challenges remain. The discrepancies found in the contribution of the A state, as well as the energetic positions and nature of the Feshbach resonance states, demand further studies of this new benchmark reaction.

References and Notes

1. W. Dong *et al*., *Science* **327**, 1501–1502 (2010).
2. M. Qiu *et al*., *Science* **311**, 1440–1443 (2006).
3. C. Xiao *et al*., *Science* **333**, 440–442 (2011).
4. R. Brownsword, M. Hillenkamp, P. Schmiechen, H. Volpp, J. Wolfrum, *Chem. Phys. Lett.* **275**, 325–331 (1997).
5. S. Liu, X. Xu, D. H. Zhang, *J. Chem. Phys.* **136**, 144302 (2012).
6. M. Alagia *et al*., *Chem. Phys.* **207**, 389–409 (1996).
7. D. Clary, *J. Chem. Phys.* **96**, 3656–3665 (1992).
8. S. Yan, Y. T. Wu, B. Zhang, X. F. Yue, K. Liu, *Science* **316**, 1723–1726 (2007).
9. S. A. Harich *et al*., *Nature* **419**, 281–284 (2002).
10. X. Wang *et al*., *Science* **322**, 573–576 (2008).
11. L. Che *et al*., *Science* **317**, 1061–1064 (2007).
12. D. M. Neumark, *J. Chem. Phys.* **125**, 132303 (2006).
13. E. Garand, J. Zhou, D. E. Manolopoulos, M. H. Alexander, D. M. Neumark, *Science* **319**, 72–75 (2008).
14. D. E. Manolopoulos *et al*., *Science* **262**, 1852–1855 (1993).
15. P. Ricaud, F. Lefèvre, *Adv. Fluorine Sci.* **1**, 1–32 (2006).
16. D. A. Neufeld, J. Zmuidzinas, P. Schilke, T. G. Phillips, *Astrophys. J. Lett.* **488**, L141–L144 (1997).
17. M. P. Deskevich, D. J. Nesbitt, H.-J. Werner, *J. Chem. Phys.* **120**, 7281–7289 (2004).
18. J. Li, R. Dawes, H. Guo, *J. Chem. Phys.* **137**, 094304 (2012).
19. J. Li, B. Jiang, H. Guo, *J. Chem. Phys.* **138**, 074309 (2013).
20. J. Li, B. Jiang, H. Guo, *Chem. Sci.* **4**, 629–632 (2013).
21. P. S. Stevens, W. H. Brune, J. G. Anderson, *J. Phys. Chem.* **93**, 4068–4079 (1989).
22. X. Yang, X.-B. Wang, L.-S. Wang, *J. Chem. Phys.* **115**, 2889–2892 (2001).
23. Y. Ishikawa, T. Nakajima, T. Yanai, K. Hirao, *Chem. Phys. Lett.* **363**, 458–464 (2002).
24. M. Ziemkiewicz, M. Wojcik, D. J. Nesbitt, *J. Chem. Phys.* **123**, 224307 (2005).
25. M. Ziemkiewicz, D. J. Nesbitt, *J. Chem. Phys.* **131**, 054309 (2009).
26. A. M. Zolot, D. J. Nesbitt, *J. Chem. Phys.* **129**, 184305 (2008).
27. C. J. Johnson, B. B. Shen, B. L. J. Poad, R. E. Continetti, *Rev. Sci. Instrum.* **82**, 105105–105105 (2011).
28. R. E. Continetti, *Annu. Rev. Phys. Chem.* **52**, 165–192 (2001).
29. The energetics are estimated from the dissociation energy (1.136 eV) of $F^-(H_2O)$ (*30*) to form F^- + H_2O, the experimental ionization energy of F^- (3.401 eV) (*31*) to reach the F + H_2O product asymptote, and the reaction enthalpy (17.6 kcal/mol) (*26*) for the F + H_2O reaction.
30. P. Weis, P. R. Kemper, M. T. Bowers, S. S. Xantheas, *J. Am. Chem. Soc.* **121**, 3531–3532 (1999).
31. C. Blondel, P. Cacciani, C. Delsart, R. Trainham, *Phys. Rev. A* **40**, 3698–3701 (1989).

Acknowledgments: This work was supported by the U.S. Department of Energy (DE-FG03-98ER14879 to R.E.C. and DE-FG02-05ER15694 to H.G.). R.O. thanks the German Academic Exchange Service (DAAD) for a postdoctoral research fellowship. J.M. thanks the National Natural Science Foundation of China (21303110) for partial support.

Supplementary Materials

www.sciencemag.org/content/343/6169/396/suppl/DC1
Materials and Methods
Figs. S1 to S5
Tables S1 to S4
References (*32*–*47*)

21 October 2013; accepted 13 December 2013
Published online 9 January 2014;
10.1126/science.1247424

Strong Ground Motion Prediction Using Virtual Earthquakes

M. A. Denolle,[1,2] E. M. Dunham,[1,3] G. A. Prieto,[4] G. C. Beroza[1]

Sedimentary basins increase the damaging effects of earthquakes by trapping and amplifying seismic waves. Simulations of seismic wave propagation in sedimentary basins capture this effect; however, there exists no method to validate these results for earthquakes that have not yet occurred. We present a new approach for ground motion prediction that uses the ambient seismic field. We apply our method to a suite of magnitude 7 scenario earthquakes on the southern San Andreas fault and compare our ground motion predictions with simulations. Both methods find strong amplification and coupling of source and structure effects, but they predict substantially different shaking patterns across the Los Angeles Basin. The virtual earthquake approach provides a new approach for predicting long-period strong ground motion.

Sedimentary basins amplify and extend the duration of strong shaking from earthquakes (*1*). State-of-the-art simulations of wave propagation for scenario earthquakes through crustal structures that include sedimentary basins explore these effects (*2*–*7*). Evidence that strong basin amplification in Los Angeles for earthquakes that would occur on the southern San Andreas fault emerged from such ground motion simulations (*3*, *7*), but because of the absence of recent earthquakes large enough to excite long-period seismic waves, they have not been validated with observations. Our study was motivated by the need to validate these simulations, which, if correct, would greatly increase seismic hazard.

To validate ground motion simulations without recordings of large earthquakes, we developed

[1]Department of Geophysics, Stanford University, 397 Panama Mall, Stanford, CA 94305, USA. [2]Scripps Institution of Oceanography, University of California, San Diego, La Jolla, CA 92093, USA. [3]Institute for Computational and Mathematical Engineering, Stanford University, Stanford, CA 94305, USA. [4]Department of Earth, Atmospheric and Planetary Science, Massachusetts Institute of Technology, 77 Massachusetts Avenue, Cambridge, MA 02139, USA.
*Corresponding author. E-mail: mdenolle@stanford.edu.

Science

Imaging Dynamics on the F + H_2O → HF + OH Potential Energy Surfaces from Wells to Barriers

Rico Otto, Jianyi Ma, Amelia W. Ray, Jennifer S. Daluz, Jun Li, Hua Guo and Robert E. Continetti

Science **343** (6169), 396-399.
DOI: 10.1126/science.1247424originally published online January 9, 2014

A View from the Middle

The intuitive way to study a bimolecular reaction is to induce a collision between separate reagents and then track the ensuing events. Crossed molecular beam studies have revealed the quantum mechanical details of numerous systems in this fashion. **Otto *et al.*** (p. 396, published online 9 January) applied a more recent approach of starting in the middle of the F + H_2O → HF + OH reaction trajectory, postcollision, by photodetaching an electron from a stabilized complex of water and a fluoride ion, and then tracking the fate of the neutral fragments.